

PCCP

Accepted Manuscript



This is an *Accepted Manuscript*, which has been through the Royal Society of Chemistry peer review process and has been accepted for publication.

Accepted Manuscripts are published online shortly after acceptance, before technical editing, formatting and proof reading. Using this free service, authors can make their results available to the community, in citable form, before we publish the edited article. We will replace this *Accepted Manuscript* with the edited and formatted *Advance Article* as soon as it is available.

You can find more information about *Accepted Manuscripts* in the [Information for Authors](#).

Please note that technical editing may introduce minor changes to the text and/or graphics, which may alter content. The journal's standard [Terms & Conditions](#) and the [Ethical guidelines](#) still apply. In no event shall the Royal Society of Chemistry be held responsible for any errors or omissions in this *Accepted Manuscript* or any consequences arising from the use of any information it contains.



PCCP

PAPER

Thermoelectricity in Polymer Composites due to Fluctuations Induced Tunneling

T. Stedman,^a K. Wei,^a G. S. Nolas^a and L. M. Woods^{*a}Received 00th January 20xx,
Accepted 00th January 20xx

DOI: 10.1039/x0xx00000x

www.rsc.org/

Transport in heavily-doped polymer composites, characterized by localized charge regions, is examined in light of the recent interest of polymers for thermoelectric applications. The developed fundamental transport theory describes carrier tunneling between charged localizations by taking into account thermally induced fluctuations of the applied potential. A range of characteristic behaviors corresponding to experimental data are described. Deviations from the Wiedemann-Franz law are also identified. This novel theory enables the determination of factors dominating the transport in polymers and a comparison to tunneling without thermal fluctuations is also provided. The obtained asymptotic expressions for the conductivity, Seebeck coefficient, and carrier thermal conductivity are particularly useful for elucidating possible routes for thermoelectric transport control and optimization.

Introduction

Pursuing alternative routes for energy conversion is at the forefront of many scientific and technological developments. The goal is to find processes and materials that are environmentally safe to reduce our reliance on fossil fuels. Thermoelectricity offers the possibility of heat driven solid-state energy conversion and power generation¹⁻³. Thermoelectric (TE) devices are especially attractive since they are reliable and environmentally safe. Their efficiency is directly related to the transport properties of the materials via the dimensionless figure of merit, $ZT = \sigma S^2 T / \kappa$ (where S is the Seebeck coefficient; σ is the carrier conductivity; $\kappa = \kappa_e + \kappa_L$ is the thermal conductivity with electronic and lattice contributions, and T is the temperature). Larger ZT values result in more efficient TE devices. Most TE materials, however, are expensive, composed of heavy or toxic elements and are not easily scalable¹⁻⁴.

These economic and safety concerns have stimulated the exploration of organic materials for TE applications. Polymers, in particular, are mechanically flexible, nontoxic, and inexpensive to process¹⁻⁵. They have an inherently low κ , much desired for high ZT , which can be at least an order of magnitude lower than that of a good inorganic TE material^{3,4,6,7}. Conducting polymers also allow for the possibility of increasing their conductivity by several orders of magnitude via doping with charge carriers while maintaining low κ values^{3,8,9,10}. It has recently been reported that $ZT \cong 0.25$ at room temperature for certain PEDOT:PSS composites^{11,12}. This is quite promising as it shows the potential for tunability, even though currently ZT is modest compared to $ZT \cong 1 - 1.5$ for inorganics^{3,4,6}.

In order to develop effective ways to optimize the TE characteristics in conducting polymers it is imperative to have a fundamental understanding of their properties and transport

mechanisms. Studies have shown that although such polymers are conducting, their transport is different than that of inorganic compounds. The nature of the π -bonding along the chain, distortion, disorder, and temperature influence transport in polymers in profound ways. Doping these materials introduces carriers that become trapped in these chains and form polarons and bi-polarons^{3,13}, which represent coupling between charge and distortion in the chain. The transport is facilitated via hopping between such quasi-particles^{3,14}. For heavily-doped polymers, however, large conducting segments comprised of many polarons are formed and tunneling between them is responsible for the transport^{3,14}. If the electrostatic charging energy is much smaller than $k_B T$ tunneling occurs providing there is an overlap between the wavefunctions of the conducting regions. This picture is similar to that of granular composites, in which tunneling occurs through the grain boundaries^{15,16}.

As T increases a second factor becomes relevant; the voltage across the boundary experiences thermal fluctuations which can stimulate tunneling. The fluctuation-induced tunneling conductivity is associated with $\sigma = \sigma_t e^{-T_t/(T+T_s)}$ (where σ_t , T_t , and T_s are effective parameters) and has been shown to be appropriate for heavily-doped organic semiconductors and disordered materials^{14,16-21}. Much of the existing work on heavily-doped polymers is interpreted in terms of this expression for σ . The Seebeck coefficient is also fit with adjustable parameters from experiment. There are no such expressions available for κ_e .

Nevertheless, a consistent transport theory focusing on this type of mechanism with *all involved carrier transport* characteristics derived on equal footing is lacking. In addition, being able to include thermal fluctuations tunneling and compare with standard tunneling broadens the fundamental understanding of transport as well as the important factors for thermoelectricity in non-crystalline media. The purpose of this paper is to address these mechanisms by establishing a

^a University of South Florida, Physics Department, Tampa, FL 33620

*Email: lmwoods@usf.edu

Electronic Supplementary Information (ESI) available: [details of any supplementary information available should be included here]. See DOI: 10.1039/x0xx00000x

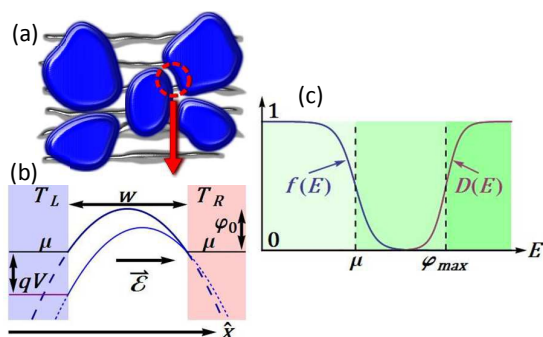


Figure 1 (Color online) (a) Schematics of heavily-doped polymers with conducting regions (blue). (b) Energy diagram of a junction of width w . The potential barrier is taken to be parabolic with a height ϕ_0 . The Fermi level is μ and T_L and $T_R > T_L$ denote the temperature on the left and right sides. The applied electric field \mathcal{E} lowers the left side by qV . (c) Fermi function $f(E)$ and tunneling probability $D(E)$ vs energy E , where $\phi_{max} = \phi_0 \left(1 - \frac{qV}{4\phi_0}\right)^2$.

complete theory for carrier transport in heavily-doped polymers. Taking into account voltage thermal fluctuations, herein we determine how σ , S and κ_e evolve as a function of T and other properties. Tunneling without such fluctuations is also considered for comparison. This novel theory reveals, in detail, the potential to control transport in polymers through tunneling and identify effective ways to interpret experimental data.

Transport Theory

The system under consideration consists of heavily-doped polymer chains with localized conducting formations throughout (Fig. 1a). When in close proximity, such localizations form a junction with an interface barrier height ϕ_0 (Fig. 1b). An applied external electric field lowers the chemical potential on the left side μ by qV (q is the charge and $V = \mathcal{E}w$). The tunneling process between the conducting regions can be affected significantly by thermal fluctuations¹⁶. This mechanism is associated with the well-known Johnson-Nyquist noise²² and is due to thermally induced voltage fluctuations caused by fluctuating excess or deficit charge at the junction resulting in a local field $\mathcal{E}_T \hat{x}$ across it. Because of the large surface area and small width of the conducting regions, the effect of \mathcal{E}_T can be quite large as compared to that of \mathcal{E} . The junction essentially behaves as a parallel plate capacitor with the probability for generating \mathcal{E}_T being $P(\mathcal{E}_T) = \left(\frac{2\varepsilon_0 w A}{\pi k_B T}\right)^{1/2} e^{(-\varepsilon_0 w A \mathcal{E}_T^2 / 2k_B T)}$, where A is the overlap area and ε_0 is the permittivity. It was shown that the Johnson-Nyquist noise dominates the transport due to thermal fluctuations and out of equilibrium contributions are secondary²³.

A polymer composite consists of many large conducting regions and is beyond the percolation threshold. To describe the transport due to tunneling through the many junctions (Fig. 1), therefore, we utilize an effective medium theory (EMT) for an inhomogeneous system perturbed by an applied external electric field and temperature gradient²⁴. Using this approach, σ , S , κ_e are calculated due to junctions with average parameters, which may be

specified from experiments. The basic assumption of the EMT is that the transport in an inhomogeneous system, beyond the percolation limit, can be described as a result of “effective” or “average” transport in a homogeneous medium²⁴.

The charge and heat currents determine the transport across the junction. Here we use a Landauer-type formalism for charge carriers with a parabolic energy dispersion $E = \frac{\hbar^2 k^2}{2m}$ (m is the effective mass)^{7,25}. The charge current through the junction j and the heat currents entering the left reservoir j_L^q and leaving the right reservoir j_R^q are

$$j = 2 \int_{-\infty}^{\infty} dE [f_R(E, \mu_R, T_R) - f_L(E, \mu_L, T_L)] M(F, E) \quad (1)$$

$$j_{L,R}^q = 2 \int_{-\infty}^{\infty} dE [f_R(E, \mu_R, T_R) - f_L(E, \mu_L, T_L)] [E - \mu_{L,R}] M(F, E) \quad (2)$$

$$M(F, E) = \frac{qm}{(2\pi)^2 \hbar^3} \int_{-\infty}^E D(F, E_x) dE_x \quad (3)$$

where $f_R(E, \mu_R, T_R)$ and $f_L(E, \mu_L, T_L)$ are the Fermi distribution functions, $\mu_{L,R}$ are the Fermi levels of the left and right reservoirs respectively (Fig. 1). $D(F, E)$ is the carrier tunneling probability in the presence of a net electric field $F = \mathcal{E} \pm \mathcal{E}_T$ and refers to the fluctuation-induced field \mathcal{E}_T pointing to the right (+) with $\mu_L = \mu - ew(\mathcal{E}_T + \mathcal{E})$ and $\mu_R = \mu$ or left (-) with $\mu_L = \mu$ and $\mu_R = \mu - ew(\mathcal{E}_T - \mathcal{E})$ ²⁶.

To account for the two equally probable orientations of \mathcal{E}_T , the currents are averaged accordingly, $\bar{j} = [j(\mathcal{E} + \mathcal{E}_T, \nabla T) + j(\mathcal{E} - \mathcal{E}_T, \nabla T)]/2$ and $\bar{j}_{L,R}^q = [j_{L,R}^q(\mathcal{E} + \mathcal{E}_T, \nabla T) + j_{L,R}^q(\mathcal{E} - \mathcal{E}_T, \nabla T)]/2$, thus the heat current through the junction \bar{j}^q results from \bar{j}_L^q and \bar{j}_R^q as $\bar{j}^q = [\bar{j}_L^q(\mathcal{E} + \mathcal{E}_T, \nabla T) + \bar{j}_R^q(\mathcal{E} - \mathcal{E}_T, \nabla T)]/2$. The thermal quantities are also averaged over $P(\mathcal{E}_T)$ yielding $J = \langle \bar{j} \rangle$ and $J^q = \langle \bar{j}^q \rangle$. The thermal averaging of any quantity $H(\mathcal{E}_T)$ is done in a standard way^{16,17} according to

$$\langle H \rangle = \left(\frac{2\varepsilon_0 w A}{\pi k_B T}\right)^{1/2} \int_0^{\infty} H(\mathcal{E}_T) e^{(-\varepsilon_0 w A \mathcal{E}_T^2 / 2k_B T)} d\mathcal{E}_T. \quad (4)$$

To obtain the carrier transport properties we apply linear response theory

$$J = \langle \mathcal{L}_{11} \rangle \mathcal{E} + \langle \mathcal{L}_{12} \rangle \nabla T, \quad J^q = \langle \mathcal{L}_{21} \rangle \mathcal{E} + \langle \mathcal{L}_{22} \rangle \nabla T \quad (5)$$

where $\mathcal{L}_{11} = \left. \frac{\partial J}{\partial \mathcal{E}} \right|_{\mathcal{E}=0} = 2 \left. \frac{\partial L_1}{\partial \mathcal{E}_T} \right|_{\nabla T=0}$, $\mathcal{L}_{12} = \left. \frac{\partial J}{\partial \nabla T} \right|_{\mathcal{E}=0} = w \left. \frac{\partial L_2}{\partial T} \right|_{\mathcal{E}=0}$, $\mathcal{L}_{21} = \left. \frac{\partial j^q}{\partial \mathcal{E}} \right|_{\mathcal{E}=0} = 2 \left. \frac{\partial L_1^q}{\partial \mathcal{E}_T} \right|_{\nabla T=0}$, $\mathcal{L}_{22} = \left. \frac{\partial j^q}{\partial \nabla T} \right|_{\mathcal{E}=0} = w \left. \frac{\partial L_2^q}{\partial T} \right|_{\mathcal{E}=0}$. The main details of the linear response theory calculations with L_1 , L_2 , L_1^q , L_2^q given in the Appendix.

The transport properties are then expressed as $\sigma = \langle \mathcal{L}_{11} \rangle$, $S = -\frac{\langle \mathcal{L}_{12} \rangle}{\langle \mathcal{L}_{11} \rangle}$ and $\kappa_e = \langle \mathcal{L}_{22} \rangle - \frac{\langle \mathcal{L}_{12} \rangle \langle \mathcal{L}_{21} \rangle}{\langle \mathcal{L}_{11} \rangle}$. The essential component here is the tunneling probability integral $M(\mathcal{E}, E)$ determined by the properties of the junction region. Its evaluation relies on $\varphi(x)$. For a parabolic barrier $\varphi(x) = 4\phi_0 \frac{x}{w^2} (w-x) - qV \frac{(w-x)}{w} + \mu$ (Fig. 1) the tunneling probability $D(\mathcal{E}, E)$ can be determined exactly²⁷. The tunneling integral (Eq. 3) can also be found

$$M(\mathcal{E}, E) = \frac{\phi_0 q m}{\gamma \pi^2 \hbar^3} \text{Log} \left[e^{\frac{\gamma}{\phi_0} (E - \varphi_{max})} + 1 \right] \quad (6)$$

where $\gamma = \pi w \sqrt{m \phi_0} / 2 \hbar^2$ is the tunneling parameter. The advantage of the parabolic barrier is that it enables finding analytical expressions for different asymptotic regimes, as shown in what follows.

	w (nm)	A (nm ²)	φ_0 (eV)	m/m_0		w (nm)	A (nm ²)	φ_0 (eV)	m/m_0
Our Data	15.567	0.618	1.329	0.00127	(A)	7	70	0.025	1
Ref.[12]	2.39	5	0.375	0.008	(B)	1	2	0.025	1
Ref.[28]	1.5	1.7	0.3	1	(C)	2	4	0.1	1
Ref.[9], ■	1.38	2.5	0.055	0.82	(D)	1	2	0.125	1
Ref.[9], ★	1.05	1.3	0.425	0.8	(E)	2.5	50	0.125	1

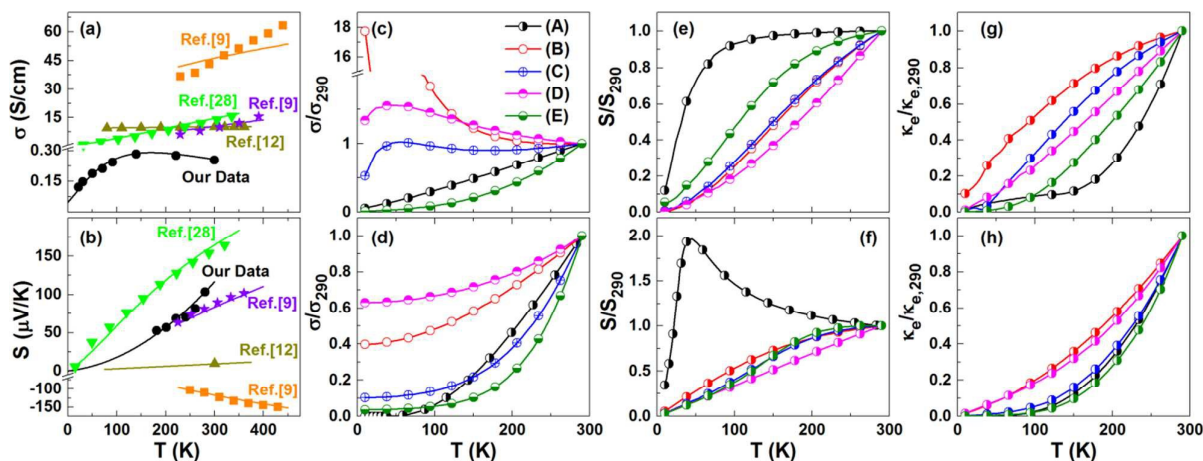


Figure 2 (Color Online) Experimental (discrete symbols) and calculated (full line) for (a) σ , (b) S vs. T . Calculated (c) σ/σ_{290} , (e) S/S_{290} , (g) $\kappa_e/\kappa_{e,290}$ vs. T for tunneling with thermal voltage fluctuations. Calculated (c) σ/σ_{290} , (e) S/S_{290} , (g) $\kappa_e/\kappa_{e,290}$ vs. T for standard tunneling. σ_{290} , S_{290} , $\kappa_{e,290}$ —conductivity, Seebeck coefficient, and thermal conductivity at $T=290$ K. Utilized parameters are summarized above and they are in the range of previously reported data¹⁶⁻²¹. Experimental data: PEDOT-PSS (5% DEF) (Ref. 12); semiconducting single-wall nanotubes (Ref. 28); poly(K_x [Ni-ett]) (Ref. 9, ■); poly(Cu_x [Ni-ett]) (Ref. 9, ★).

Properties of the Fluctuation-Induced Tunneling

The transport properties can now be calculated numerically using Eqs. (1-6) for specified w , A , φ_0 and m . First we validate the model by describing several reported measurements, as shown in Fig. 2^{9,12,28}. For each case, numerically scanning the values for w , A , φ_0 and m to obtain the best possible fit between the experimental data and the calculations is done. The measurement results for “Our data” correspond to Poly(3,4-ethylenedioxythiophene)-poly(styrenesulfonate) (PEDOT:PSS, 3-4% in water) purchased from Alorich and used without further processing. The solution was dried inside a vacuum oven under 35°C for 12h and then ground in liquid nitrogen to fine powder. For densification the powders were hot pressed into a pellet using custom-designed 12 mm diameter graphite tooling at 100°C and 45 MPa for 1 h under N_2 flow. Temperature dependent four-probe resistivity, ρ , Seebeck coefficient, S (gradient sweep method) and steady-state κ measurements were conducted in a custom designed radiation-shielded vacuum probe with uncertainties of 4, 6, and 8% for ρ , S , and κ measurements¹⁵, respectively, on $2 \times 2 \times 5$ mm³ parallelepipeds cut by a surgical knife.

The theory is also applied to other report measured data on a variety of polymer composites. Figs. 2a,b shows that there is good agreement between the calculations and experimental measurements for PEDOT-PSS (our data), PEDOT-PSS¹², metal-coordinated polymers⁹, and carbon nanotube composites²⁸⁻³⁰. The fact that the σ , S vs T behavior is reproduced for a range of polymer composites shows that thermally induced voltage fluctuations are relevant and that our theory captures the transport.

The variation in the measured data for many types of polymers^{1-5,9-12} is described by this model and shown in Figs. 2c, e, g, where σ , S , κ_e vs. T for different junction parameters are presented. The junction parameters affect the transport quite dramatically. This is much more apparent in σ , which can have linear increase, decrease or a local maximum vs T . S can be affected primarily in terms of its magnitude and the characteristics of its maximum value (Fig.2e). The thermal conductivity typically increases nonlinearly as a function of T (Fig. 2g). We note that several experimental studies for σ have been interpreted in terms of the fluctuation-induced tunneling as estimates for the junctional parameters have also been given^{8,16-21}. For example, the barrier heights are found in the 1-1000 meV range, the overlap areas are in the 0.1-100 nm² intervals, while w is found to be in the nm scale. This variation can be attributed to the different types of polymers and synthesis and processing techniques used. The tunneling characteristics in Fig.2 are in within the experimentally reported ranges.

Measurements for σ in heavily-doped polymers are often interpreted in terms of fluctuation-induced tunneling, however, S is described by a heterogeneous model invoking additional factors such as polaron hopping or disorder⁸. This is unusual as to why different mechanisms are important for one property, but not for the other. We see that the comprehensive theory developed here explains the nonmetallic behavior of σ and the metallic-like behavior for S without invoking other factors preferentially. Moreover, in agreement with reported experimental data^{1-5,8,12}, our calculations show a plethora of σ vs. T types of functionalities while S vs. T retains metallic-like behavior.

Table I. The low and high T expressions for σ , κ_e , S , and the Lorentz number $L = \kappa_e/\sigma T$ for thermal fluctuations and standard tunneling are given. The parameters T_0 , T_1 , and α are also

	Tunneling with Thermal Fluctuations		Standard Tunneling	
	Low T	High T	Low T	High T
σ	$\frac{w\varphi_0 q^2 m}{2\gamma\pi^2 \hbar^3} \left(\frac{T_0}{T+T_0}\right)^{3/2} e^{-\frac{T_1}{T+T_0}}$	$\frac{wq^2 m k_B}{2\pi^2 \hbar^3} \left(\frac{\alpha}{1+\alpha}\right)^{3/2} T e^{-\frac{1}{T(1+\alpha)}}$	$\frac{w\varphi_0 q^2 m}{2\gamma\pi^2 \hbar^3} e^{-\gamma}$	$\frac{wq^2 m k_B}{\pi^2 \hbar^3} T e^{-\frac{\varphi_0}{k_B T}}$
κ_e	$\left(\frac{w\varphi_0 m k_B^2}{6\gamma \hbar^3}\right) T \sqrt{\frac{T_0}{T+T_0}} e^{-\frac{T_1}{T+T_0}}$	$\frac{w m k_B^3}{\pi^2 \hbar^3} \left(\frac{\alpha}{1+\alpha}\right)^{3/2} T^2 e^{-\frac{1}{T(1+\alpha)}}$	$\frac{w\varphi_0 m k_B^2}{6\gamma \hbar^3} T e^{-\gamma}$	$\frac{w m k_B^3}{\pi^2 \hbar^3} T^2 e^{-\frac{\varphi_0}{k_B T}}$
S	$-\frac{\gamma\pi^2 k_B^2}{3q\varphi_0} T \left(1 + \frac{T}{T_0}\right)$	$-\frac{2k_B}{q} \left(1 + \frac{5}{4\alpha}\right)$	$-\frac{\gamma\pi^2 k_B^2}{3q\varphi_0} T$	$-\frac{2k_B}{q}$
L	$\frac{\pi^2 k_B^2}{3q^2} \left(1 + \frac{T}{T_0}\right)$	$\frac{2k_B^2}{q^2}$	$\frac{\pi^2 k_B^2}{3q^2}$	$\frac{k_B^2}{q^2}$
Effective parameters	$T_1 = \frac{8\varepsilon_0 \varphi_0^2 A}{k_B q^2 w}$		$\alpha = \frac{k_B T_1}{\varphi_0}$	$T_0 = \frac{T_1}{\gamma}$

Eqs. (1-6) are also suitable to describe tunneling when thermal fluctuations are not present. Simply taking the probability $P(\mathcal{E}_T) = \delta(\mathcal{E}_T)$, the properties without thermal fluctuations can be calculated (Fig. 2d,f,h). Figs. 2d,c show that the non-monotonic behavior of tunneling with thermal fluctuations is quite different than the nonlinear σ for standard tunneling. Figs. 2e,f show that S has similar behavior however the magnitude for standard tunneling is smaller. κ_e vs. T is also similar for both mechanisms while κ_e is larger for standard tunneling (Fig. 2g,h).

The general theory described in Eqs. (1-6) can further be analyzed by obtaining analytical expressions for low and high T regimes for both types of tunneling. For this purpose, the tunneling integral is approximated as

$$M(\mathcal{E}, E) = \begin{cases} \frac{\varphi_0 e m}{\gamma(2\pi)^2 \hbar^3} e^{\frac{\gamma}{\varphi_0}(E - \varphi_{max})} & , E < \varphi_{max} \\ \frac{e m}{(2\pi)^2 \hbar^3} (E - \varphi_{max}) & , E > \varphi_{max} \end{cases} \quad (7)$$

The transport properties for low T are found by using the Sommerfeld expansion for the integrals in L_1 , L_2 , L_1^q , L_2^q , valid for $\frac{\varphi_0}{\gamma} > k_B T$. For high T , where $\frac{\varphi_0}{\gamma} < k_B T$, most carriers are thermally activated meaning that they have energy larger than the Fermi level. Thus we utilize the Boltzmann distribution approximation $f(E, \mu, T) = e^{-\frac{E-\mu}{k_B T}}$ for $E > \mu$ and consider only transport from carriers with energies above μ . As a result, the characteristics are found analytically and summarized in Table I.

The analytical σ , κ_e , and S capture the transport behavior in a more transparent manner. These results enable an interpretation in terms of a balance between the decreasing $f_{L,R}$ weighted against an increasing $D(\mathcal{E}, E)$, as shown in Fig. 1c. The carriers with $E > \mu$ correspond to the thermally activated regime appropriate for high T . The low-energy carriers with $E < \mu$ mainly tunnel through and responsible for the low T transport. The key factors for the non-monotonic behavior in Fig. 2a, c come from the different T -dependence of the prefactors for the low T and high T σ together and the tunneling parameters. For standard tunneling, however, the T -dependence is rather typical with an increasing behavior captured by the high T expression in σ (also, Fig. 2d). We further see that the S vs T function for both processes is similar, however the T^2 function and the larger high T saturation value result in larger Seebeck coefficient for the fluctuations tunneling. The analytical results show that the tunneling parameters do not affect the transport properties independently. The influence of each parameter depends on the rest of the tunneling characteristics

via the prefactors, T_0 , T_1 , α making the description sometimes complex.

The Wiedemann-Franz (WF) law is also of interest for transport. It shows that thermal and electrical currents are carried by the same quasiparticles and relates σ and κ_e through the Lorentz number $L_0 = \kappa_e/\sigma T = \pi^2 k_B^2/3q^2$. This relation is often utilized in experiments to separate κ_e and κ_L . Marked deviations from the WF law happen in structures with reduced dimensions³¹. Deviations from L_0 are also found here. The analytical expressions (Table I) show the WF law for low T is given by $L = L_0(1 + T/T_0)$. For high T , L is a fraction of the Lorentz number - $L = 6L_0/\pi^2$. Regular tunneling preserves L_0 at low T , however for high T the WF law is modified, $L = 3L_0/\pi^2$.

Conclusions

In this paper, carrier transport in heavily-doped polymers is considered. We establish a comprehensive theory for the charge carrier properties as a result of tunneling between localized conducting regions in the polymer chains and facilitated by thermal fluctuations. The characteristic behavior of the nonmetallic σ and metallic-like S agrees well with numerous experimental data. This approach can also be relevant to carbon nanotube composites²⁸⁻³⁰. Calculating the transport characteristics by consistent examination of the parameters in the theoretical model can provide guidelines for a composite with desired thermoelectric properties. The analytical asymptotic expressions are useful for an in-depth analysis of important factors limiting the transport and finding ways to modulate the transport. Comparisons with standard tunneling and the WF law deviations bring further merit to this complete theory, and will be of particular importance to experimentalists seeking pathways for data interpretation and pathways to enhancing thermoelectricity of polymer materials.

Acknowledgements

This work was supported by the National Science Foundation under Contract No. DMR-1400957. K.W. gratefully acknowledges financial support from the II-VI Foundation. The authors are grateful for discussions with Prof. David Cahill.

References

- N. Dubey and M. Leclerc, *J. Polym. Sci., Part B: Polym. Phys.*, 2011, **49**, 467-475.
- Y. Du, S. Z. Shen, K. Cai and P. S. Casey, *Prog. Polym. Sci.*, 2012, **37**, 820-841.
- O. Bubnova and X. Crispin, *Energy Environ. Sci.*, 2012, **5**, 9345-9362.
- T. O. Poehler and H. E. Katz, *Energy Environ. Sci.*, 2012, **5**, 8110-8115.
- D. Wang, W. Shi, J. Chen, J. Xi and Z. Shuai, *Phys. Chem. Chem. Phys.*, 2012, **14**, 16505-16520.
- J. Liu, X. Wang, D. Li, N.E. Coates, R. A. Segalman and D. G. Cahill, *Macromol.*, 2015, **48**, 585-591.
- Y. Wang, J. Liu, J. Zhou, and R. Yang, *J. Phys. Chem. C*, 2013, **117**, 24716.
- A. B. Kaiser, *Adv. Mater.*, 2011 **13**, 927-941.
- J. Yang, H. Yip and A. K.-Y. Jen, *Adv. Energy Mater.*, 2013, **3**, 549-565.
- X. Gao, K. Uehara, D.R. Klug, S. Patchkovskii, J.S. Tse, and T.M. Tritt, *Phys. Rev. B*, 2005, **72**, 125202.
- O. Bubnova, Z. U. Khan, A. Malti, S. Braun, M. Fahlman, M. Berggren and X. Crispin, *Nat. Mater.*, 2011, **10**, 429-433.
- O. Bubnova, Z.U. Khan, H. Wang, S. Braun, D. R. Evans, M. Fabretto, P. Hojati-Talemi, D. Dagnelund, J.-B. Arlin, Y. H. Geerts, S. Desbief, D. W. Breiby, J. W. Andreasen, R. Lazzaroni, W. M. Chen, I. Zozoulenko, M. Fahlman, P. J. Murphy, M. Berggren and X. Crispin, *Nat. Mater.*, 2014, **13**, 190-194.
- J. L. Brédas and G. B. Street, *Acc. Chem. Res.*, 1985, **18**, 309-315.
- A. B. Kaiser and V. Skákalova, *Chem. Soc. Rev.*, 2011, **40**, 3786-3801.
- A. Popescu, L. M. Woods, J. Martin and G. S. Nolas, *Phys. Rev. B*, 2009, **79**, 205302; J. Martin, L. Wang, L. Chen and G. S. Nolas, *Phys. Rev. B*, 2009, **79**, 115311.
- P. Sheng, *Phys. Rev. B*, 1980, **21**, 2180-2195.
- E. K. Sichel, P. Sheng, J. I. Gittleman and S. Bozowski, *Phys. Rev. B*, 1981, **24**, 6131-6134.
- J. Ederth, P. Johnsson, G. A. Niklasson, A. Hoel, A. Hultåker, P. Heszler, C. G. Graqvist, A. R. van Doom, M. J. Jongerius and D. Burgard, *Phys. Rev. B*, 2003, **68**, 155410.
- S. Mitra, S. Banerjee and D. Chakravorty, *J. Appl. Phys.*, 2013, **113**, 154314.
- J. Syurik, O. A. Ageev, D. I. Cherednichenko, B. G. Konoplev and A. Alexeev, *Carbon*, 2013, **63**, 317-323.
- M. Salvato, M. Cirillo, M. Lucci, S. Orlanducci, I. Ottaviani, M. L. Terranova and F. Toschi, *Phys. Rev. Lett.*, 2008, **101**, 246804.
- J. Johnson, *Phys. Rev.*, 1928, **32**, 97-109; H. Nyquist, *Phys. Rev.*, 1928, **32**, 110-113.
- I. V. Krive, E. N. Bogachek, A. G. Scherbakov and U. Landman, *Phys. Rev. B*, 2001, **64**, 233304.
- S. Kirkpatrick, *Rev. Mod. Phys.*, 1973, **45**, 574-588; I. Webman, J. Jortner and M. Cohen, *Phys. Rev. B*, 1977, **16**, 2959-2964; J. Bernasconi, *Phys. Rev. B*, 1973, **7**, 2252-2260.
- Y. V. Nazarov and Y. M. Blanter, *Quantum Transport: Introduction to Nanoscience*, Cambridge University Press, Cambridge, 2009, ch 1.
- Note that the Fermi level μ is related to the carrier concentration n_c of the polymer composite via the standard relation $n_c = \int_{-\infty}^{\infty} g(E) dE / (1 + \exp((E - \mu)/k_B T))$, where $g(E)$ is the density of states.
- L. D. Landau and E. M. Lifshitz, *Quantum Mechanics. Non-Relativistic Theory*, Pergamon Press, Oxford, 3rd edn, 1977, ch. 7.
- Y. Nakai, K. Honda, K. Yanagi, H. Kataura, T. Kato, T. Yamamoto and Y. Maniwa, *Appl. Phys. Express*, 2014, **7**, 025103.
- L. An, W. Xu, S. Rajagopalan, C. Wang, H. Wang, Y. Fan, L. Zhang, D. Liang, J. Kapat, L. Chow, B. Guo, J. Liang, and R. Vaidyanathan, *Adv. Mat.*, 2004, **16**, 20036-20040.
- The transport of many carbon nanotube composites is similar to the transport of polymers^{1,8,9,14,16}. Researchers have attributed the presence of a giant Seebeck coefficient to tunneling between carbon nanotubes^{28,29} and the model we have developed captures the characteristic behavior. This is indicative again of the similarities between polymers and carbon nanotube composites.
- B. Kubala, J. König and J. Pekola, *Phys. Rev. Lett.*, 2008, **100**, 066801.